Submitted, accepted and published by:
International Journal of Greenhouse Gas Control 5 (2011) 659–667

High temperature behaviour of a $CuO/\gamma Al_2O_3$ oxygen carrier for Chemical-Looping Combustion

***Forero C.R.*[1], Gayán P.[2], García-Labiano F.[2], de Diego L.F.[2], Abad A.[2], and Adánez J.[2]**

1 University of Valle, Engineering School of Natural and Environmental Resources (EIDENAR). Calle 13 No. 100-00, 25360 Cali, Colombia, e-mail: caforero@univalle.edu.co. Fax: (+34) 976 733 318.

2 Instituto de Carboquímica (CSIC), Dept. of Energy & Environment, Miguel Luesma Castán, 4, Zaragoza, 50018, Spain.

Corresponding author: Tel: (+34) 976 733 977. Fax: (+34) 976 733 318. E-mail address: crforero@icb.csic.es (Carmen Rosa Forero)

Abstract

Chemical-Looping Combustion (CLC) is a combustion technology with inherent CO_2 separation and, therefore, without energy losses. CLC is based on the transfer of oxygen from the air to the fuel by means of an oxygen carrier (OC) in the form of a metal oxide. The OC circulates between two interconnected reactors, the fuel (FR) and the air reactor (AR). To scale up the CLC process for industrial application OCs materials suitable to work at high temperatures are needed. So far, Cu-based OCs had been proved to fulfil the requirements for an OC material, although operating temperatures lower than 1073 K are recommended.

In this work, the behaviour of an impregnated Cu-based oxygen carrier (CuO-γAl_2O_3) was studied in a continuous CLC unit of 500 W_{th} during long-term tests using methane as fuel gas and FR temperatures up to 1173 K and AR temperatures up to 1223 K.

The behaviour of the oxygen carrier on the process performance was evaluated taking into account important aspects such as combustion efficiency, resistance to attrition, fluidization behaviour and preservation of the oxygen transport capacity and reactivity. It was found that both T_{FR} and T_{AR} had a great influence on the resistance to attrition of the particles. Stable operation for more than 60 h was only feasible at T_{FR} =1073 K and T_{AR} = 1173 K. However agglomeration or deactivation of the particles was never detected in any of the temperatures used.

This is the first time that a CuO-γAl_2O_3 OC, prepared by a commercial manufacturing method, and used at 1073K in the FR and 1173 K in the AR exhibits such a good properties: high reactivity together with high mechanical durability and absence of agglomeration. This result opens new possibilities for the application of Cu-based materials in industrial-scale CLC processes.

Keywords: CO_2 capture, chemical-looping combustion, copper.

1. Introduction

The CO_2 capture and storage (CCS) is a process involving the separation of CO_2 emitted by industry and energy-related sources, and the storage for its isolation from the atmosphere over long term, helping on this way to reduce the strongly effects of the global warming caused by this gas (IPCC, 2007). There are different CCS technologies available or under development, but most of them have high energy penalty as a consequence of the gas separation step, which results in an increase of the cost of energy production. In this context, Chemical Looping Combustion process (CLC) has been suggested among the best alternatives to reduce the

economic costs of CO_2 capture using fuel gas (Kerr, 2005) and to increase the efficiency with respect to other CO_2 capture processes (Kvamsdal et al., 2007). In this process, CO_2 is inherently separated from other combustion products, N_2 and unused O_2, through the use of a solid oxygen carrier (OC) and thus no energy is expended for the separation. The CLC process has been demonstrated for gaseous fuel combustion in 10-140 kW_{th} units using methane or natural gas and Ni- or Cu-based oxygen carriers (Ryu et al., 2005; Lyngfelt and Thunman, 2005a; Adánez et al., 2006; Linderholm et al., 2008; Kolbitsch et al., 2009a) and for syngas combustion using CoO, NiO or ilmenite as oxygen carriers (Kolbitsch et al., 2009b; Ryu et al., 2010).

A cornerstone in the successful development of a CLC system is the oxygen carrier, which besides having a sufficient oxygen transfer capacity and a high reactivity with the fuel and air for many cycles of reduction-oxidation, must meet other characteristics such as high resistance to attrition and agglomeration, long-term durability in chemical and physical integrity, good properties for fluidization-bed applications and low production cost. Moreover, full fuel conversion to CO_2 and H_2O is desired. Among the different metal oxides proposed in the literature for the CLC process, Cu-based oxygen carriers have shown high reaction rates and oxygen transfer capacity (Adánez et al., 2004), and have no thermodynamic restrictions for complete fuel conversion to CO_2 and H_2O. In addition, the use of Cu-based oxygen carriers has less environmental problems and a lower cost than other materials used for CLC process such as nickel or cobalt.

Our research group at the “Instituto de Carboquímica” (CSIC) has been developing Cu-based oxygen carriers during the last 10 years. Potential Cu-based oxygen carriers were prepared using different supports by Adánez et al. (2004). The effects of oxygen carrier composition and preparation method were also investigated in a thermobalance to develop oxygen carriers with high reaction rates and durability (de Diego et al., 2004). It was found that the optimum preparation method for Cu-based oxygen carriers was the impregnation on a resistant support.

Later, the preparation conditions and oxygen carrier characteristics were optimized to avoid the agglomeration of the Cu-based materials during their operation in a fluidized bed (de Diego et al., 2005), which was the main reason adduced in the literature to reject this kind of materials for their use in a CLC process (Copeland et al., 2002; Cho et al., 2004). Based on these findings, an oxygen carrier was finally selected to test its behaviour in a 10 kW_{th} CLC prototype using methane as fuel. The results obtained during 200 h of continuous operation were very successful both regarding methane combustion efficiencies and particle behaviour (Adánez et al., 2006; de Diego et al., 2007). A waste management study using Cu-based materials coming from this CLC plant was also carried out (García-Labiano et al., 2007). It was concluded that the solid residues generated in a CLC plant using Cu-based materials can be classified as a stable non-reactive hazardous waste, acceptable at landfills for non-hazardous wastes. Additional work has been recently carried out to test the behaviour of this oxygen carrier in a CLC continuous unit of 500 W_{th} using syngas as fuel (Forero et al., 2009) or methane containing variable amounts of light hydrocarbons (LHC) or H_2S (Gayán et al., 2010, Forero et al., 2010). It was found that the OC can fully convert syngas or methane at 1073 K. Moreover, no special measures should be adopted due to the presence of LHC in the fuel gas of a CLC plant since unburnt hydrocarbons were never detected at any experimental conditions at the fuel reactor outlet. With respect to the presence of H_2S in the fuel gas, it was found that the great majority of the sulphur fed into the system was released in the gas outlet of the FR as SO_2, affecting only to the quality of the CO_2 produced. Formation of copper sulphide, Cu_2S, and the subsequent reactivity loss was only detected working at low values of the oxygen carrier to fuel ratio ($\phi < 1.5$), although this fact did not produce any agglomeration problem in the reactors. To summarize, Cu-based OCs had been proved to fulfil the requirements for an OC material, although FR operational temperatures up to 1073 K were always used. This temperature was recommended to avoid agglomeration problems derived from the increase of the particle temperature near the melting point of metal, 1358K for Cu, taking into account that both reduction and oxidation reactions are exothermic in the case of Cu-based OCs. However, an increase in the temperature would increase the efficiency of the process.

CLC has been found as a promising technology with high energetic efficiency in power/heat generation with inherent capture of CO_2 (Kerr, 2005). CLC have also a number of possible applications in the oil and gas industry to replace conventional CO_2 capture systems in heaters and boilers for heat and steam generation. Moreover, the integration of a CLC system in the production of H_2 with CO_2 capture has also been proposed as a heat source for the methane steam reforming (Rydén et al., 2009).

There is a concern about how to integrate the CLC process in a power plant maximising the net efficiency (Ishida and Jin, 1994; Anheden and Svedberg, 1998; Jin and Ishida, 2000; Brandvoll and Bolland, 2004). Naqvi and Bolland, (2007) proposed a CLC combined cycle with a 45.1 % of net plant efficiency at 1173 K with close to 100 % of CO_2 capture. It is well known that in a thermal process, increasing the inlet gas temperature in the gas turbine increases the net efficiency of the process. An increase of 200 K in this temperature could cause an increase in the net plant efficiency until values about 49.7 %. However, same authors proposed to introduce reheat in the air turbine at relatively low and safe oxidation temperature (1173 K) resulting in a 49 % of net plant efficiency, which is higher to that of a conventional combined cycle with 90 % of post combustion CO_2 capture (48.6 %).

It is clear that to scale up the CLC technology; information about the high temperature resistance of the oxygen carriers would be needed. By temperature resistance is meant the ability to withstand high temperature without defluidizing or agglomerating, with low attrition rate and stable reactivity. Agglomeration problems are particularly important working with Cu-based OC due to the low melting temperature of the metal (1358K). In addition, the attrition rate of the oxygen carriers is another important parameter to be accounted as a criterion for using a specific material in a fluidized bed reactor. High attrition rates will decrease the lifetime of the particles increasing the cost of the CLC process.

There are in the literature very few works dealing with this aspect. de Diego et al. (2005) used a Cu-based oxygen carrier at 1223 K in a batch fluidized bed reactor during 20 reduction and

oxidation cycles. They found that the behaviour of the oxygen carrier with respect to chemical stability and reactivity was very satisfactory despite the high temperature used, although a small number of cycles were carried out. For this reason, it is necessary to advance on the study of the behaviour of the copper-based oxygen carriers at high temperatures.

The aim of this paper is to analyze the behaviour of a Cu-based oxygen carrier developed for the CLC process at higher temperature ranges than previously tested. According to a literature review, this is the first time that the performance of a Cu-based oxygen carrier is tested at temperatures higher than 1073 K during continuous operation. Long-term tests were carried out in a CLC continuous unit of 500 W_{th} using methane as fuel and a copper-based oxygen carrier at temperatures of 1073 – 1173 K in FR and 1173 – 1223 K in AR under continuous operation. Changes in particles with respect to reactivity, chemical composition and physical characteristic were analyzed. The influence of the reactors temperature and solids circulation rate on gas products distribution, combustion efficiency, attrition, and material agglomeration was investigated.

2. Experimental

2.1. Oxygen carrier

The oxygen carrier used in this work was prepared by the incipient wet impregnation method using CuO as active phase and commercial γ-Al_2O_3 (dp = 0.3-0.5 mm) as support. The method was described in detail in a previous work (Adanez et al., 2006). The main characteristics of the Cu-based oxygen carrier, Cu14Al, are showed in Table 1.

2.2. Oxygen carrier characterization

Fresh and after-used samples of the oxygen carriers were physically and chemically characterized by several techniques. The reactivity of the OC was determined by TGA technique using CH_4 as fuel (García-Labiano et al., 2004). The oxygen transport capacity, defined as the mass fraction of oxygen that can be used for the oxygen transfer, was determined by thermogravimetric analysis using H_2 as fuel. This property is calculated as $R_{o,OC} = (m_{ox} - m_{red})/m_{ox}$, where m_{ox} and m_{red} are the weights of the oxidized and reduced forms of the oxygen carrier, respectively. The particle size diameter (PSD) was determined with a LS 13 320 of Beckman Coulter equipment. The system allows the PSD determination ranging from 0.04 to 2000 microns. The bulk density of the oxygen carrier particles was calculated weighting a known volume of solid and assuming that the void was 0.45 corresponding to loosely packed bed. The specific surface area was estimated by Brunauer-Emmett-Teller method (BET) using a Micromeritics ASAP 2020. The porosity was measured by Hg intrusion in a Quantachrome PoreMaster 33. The force needed to fracture a particle was determined using a Shimpo FGN-5X crushing strength apparatus. The crushing strength was taken as the average value of at least of 20 measurements. The identification of crystalline chemical species was carried out by powder X-Ray Diffraction (XRD) in a Bruker AXS D8 Advance, equipped with monochromatic beam diffracted graphite, using Ni-filtered "Cu Kα" radiation. The microstructures of the particles and element distribution in the solid were observed by a Scanning Electron Microscopy (SEM) in a Hitachi S-3400 N, with an EDX analyzer Röntec XFlash of Si(Li). To analyze the internal section of the particles, some particles were embedded in resin, cut with a diamond blade and polished.

2.3. CLC continuous unit of 500 W_{th}

Figure 1 show a schematic diagram of the reactor system, which was designed and built at "Instituto de Carboquímica" (CSIC). The facility used in this study is a CLC continuous unit of 500 W_{th} composed of two interconnected fluidized bed reactors. Detailed information about the prototype and operating procedure used can be found elsewhere (Forero et al., 2009).

The fuel reactor (A) and the air reactor (C) are separated by a loop seal (B) to avoid mixing fuel and air. The solids from the AR are transported by a riser (D), recovered by a cyclone (E) and returned to the FR trough a solids valve (G) that controls the solid circulation rate and also acts as a loop seal. The diverting solids valve (H) can measure this circulation rate. Moreover, the composition of both outlet streams is analyzed on-line using specific gas analyzers. Fine particles produced by attrition were recovered in the filters placed downstream of both reactors. The prototype allowed the collection of solid material samples from the AR at any moment from the diverting solid valve, and from the FR at the end of the test.

The solid inventory in the plant was about of 1.2 kg of OC. The inlet gas flow in the FR was 260 L_N/h corresponding to a gas velocity of 0.14 m/s, which was about 2.5 times the minimum fluidization velocity of the particles. The fuel gas in the FR was methane diluted in nitrogen, and no steam was added. Nitrogen was used as a fluidizing agent in the bottom loop seal (45 L_N/h). Air was used as fluidizing gas in the AR. To achieve complete oxidation of the reduced oxygen carrier in the AR, the air was divided into the fluidizing gas in the bottom bed (720 L_N/h), allowing high residence times of the particles, and into the secondary air in the riser (150 L_N/h) to help particle entrainment.

2.3.1. Combustion tests

Four long-term tests under different operating conditions were carried out using Cu14Al particles and methane as fuel. A new batch of Cu14Al particles was used for each test. Table 2 shows a summary of the different operating conditions used in each test. The effect of increasing the operating temperature in the FR or in the AR on the resistance of the particles were analysed independently. The operating temperatures were varied between 1073 and 1173 K in the FR and between 1173 and 1223 K in the AR. Tests 1 and 2 were carried out at 1073 K in the FR and increasing the AR temperature up to 1173 K and 1223 K. Tests 3 and 4 were carried out at 1173 K in the FR and increasing the AR temperature up to 1173 K and 1223 K. In each test, the FR

and AR temperatures were kept constant. The duration of the tests were fixed to be long enough to analyze the effect of temperature on the physical and chemical characteristics of the particles and make a reliable estimation of the particle lifetime at those conditions. A total of about of 216 h in hot condition in the CLC continuous unit of 500 Wth, of which 182 h corresponded at combustion conditions with methane were carried out during tests 1 to 4. Tests 2, 3 and 4 had to be stopped after 42, 48, and 29 h respectively of smooth operation due to operational problems caused by the sudden increase of fines generated in these operating conditions.

Moreover, the effect of the operating conditions on the combustion efficiency was also analysed in each test. Thus, the effect of the oxygen carrier to fuel ratio, ϕ, on the combustion efficiency was carried out varying the fuel concentration but keeping all the other experimental conditions constant. It must be pointed out, that although during the first 10 h of operation the experiments were carried out at different power inputs, the solids inventory in the FR (≈ 0.2 kg) and the air flow in the AR were maintained constant. The remaining operation time was carried out at constant operating conditions corresponding to those of complete combustion of methane.

The combustion efficiency was defined as the ratio of the oxygen consumed by the gas leaving the FR to that consumed by the gas when the fuel is completely burnt to CO_2 and H_2O. So, the ratio gives an idea about how the CLC operation is close or far from the full combustion of the fuel, i.e. η_c = 100%.

$$\eta_C = \frac{\left(2x_{CO_2} + x_{CO} + x_{H_2O}\right)_{out} F_{out}}{\left(4x_{CH_4}\right)_{in} F_{in}} 100 \quad (1)$$

where F_{in} is the molar flow of the inlet gas stream, F_{out} is the molar flow of the outlet gas stream, and x_i is the molar fraction of the gas i corresponding to the inlet or outlet.

The oxygen carrier to fuel ratio (ϕ) was defined by Eq. (2), where F_{CuO} is the molar flow rate of copper oxide and F_{CH_4} is the inlet molar flow rate of the CH_4 in the FR. A value of ϕ = 1

corresponds to the stoichiometric CuO amount needed for a full conversion of the fuel to CO_2 and H_2O:

$$\phi = \frac{F_{CuO}}{4\,F_{CH_4}} \tag{2}$$

The experimental data obtained after the tests gave the combustion efficiency, η_c, obtained at each operating condition (temperature, fuel gas composition, and solid circulation rate), calculated according to Eq. (1).

3. Results and discussion

The CLC continuous unit of 500 W_{th} has been operated using Cu14Al and methane as fuel. The results are presented analyzing the influence of the FR and AR temperatures and oxygen carrier to fuel ratio on the combustion efficiency and gas products distribution and on the behaviour of the OC with respect to material agglomeration, attrition rate and particle integrity.

3.1. Combustion efficiency

To analyze the behaviour of the Cu-based oxygen carrier during methane combustion at high temperature, several tests under continuous operation were carried out at different ϕ values. Table 2 shows the main operating conditions for the experiments carried out. The steady-state for the different operating conditions was maintained at least for two hours in each test.

Fig. 2 shows the effect of the oxygen carrier to fuel ratio, ϕ, on the combustion efficiency at different temperatures both FR and AR. In all cases an increase in ϕ produces an important increase in the combustion efficiency. The fuel was fully converted working at ϕ values above 1.4 at T_{FR} = 1073 K and ϕ values above 1.2 at T_{FR} = 1173 K. When the ϕ value decreased, the combustion efficiency also decreased because of the lower oxygen availability in the FR, being this effect more noticeable at the lowest temperature (T_{FR} = 1073 K). An increase in the fuel

reactor temperature produced an increase in the combustion efficiency. This effect was due to higher oxygen carrier reactivity as a consequence of the dependence of the kinetic constant with the temperature. The increase in T_{AR} (test 3 and 4) produced a negligible effect on the combustion efficiency. This effect was because the oxygen carrier reached full oxidation state in the AR even at T_{AR} = 1173 K due to its high oxidation reactivity and solid residence time.

The loss of combustion efficiency could be due to unburnt gases CH_4, CO, and H_2 present at the outlet stream of the FR and to carbon formation in the FR. Fig. 3 shows the FR gas outlet compositions as a function of ϕ at different temperatures for CH_4, CO and H_2. It can be seen that the amount CH_4, CO and H_2 increased as the oxygen carrier to fuel ratio decreased at T_{FR} = 1073 K, independently of the AR temperature. The CH_4, CO and H_2 concentration at the FR gas outlet were negligible at T_{FR} = 1173 K.

The carbon formation process was also analyzed during continuous operation in the prototype. The carbon formed on the OC particles in the FR could be transferred to the AR and burnt giving CO and/or CO_2. In the CLC pilot plant carbon formation was evaluated by measuring the CO and CO_2 concentrations at the outlet from the AR. As there was not gas leakage from the FR to the AR, any carbon containing gas present in the AR outlet should come from combustion of the solid carbon deposited on the oxygen carrier particles. CO was never detected at the outlet of the AR in any test. Nevertheless, CO_2 was detected in the gas outlet of the AR at operating conditions of ϕ values lower than 1.2 at T_{FR}=1073-1173 K. From Fig. 2, the operating conditions corresponding to full gas combustion can be inferred (ϕ >1.4 at 1073 K or ϕ > 1.2 at 1173 K). These conditions are also those corresponding to operation without carbon formation. These results agreed with those found in previous work working with this OC and methane or syngas as fuel gas (Adánez et al., 2006; Forero et al., 2009).

3.2. Oxygen carrier behaviour

Satisfactory results regarding the combustion of methane at T_{FR} =1173 K, and T_{AR} > 1173 K were obtained. However, other aspects like agglomeration, attrition, reactivity, and oxygen carrier properties should be taken into account to evaluate the behaviour of the oxygen carrier during long-term tests at high temperature.

3.2.1. Agglomeration

As discussed above, the oxygen carriers based on copper have been rejected as candidates for the CLC system because could present agglomeration problems (Copeland et al., 2002; Cho et al., 2004). Despite this background, de Diego et al. (2005) found suitable preparation conditions to avoid this phenomenon and thus take benefit of its main advantages: high oxygen transport capacity and reactivity, complete combustion to CO_2 and H_2O without producing CO or H_2, exothermic reactions both in oxidation and in reduction, together with a moderate cost and low toxicity. The Cu-based OC used in this work was manufactured following the preparation conditions that avoid agglomeration problems indicated by de Diego et al., 2005, that is, low CuO content (<20%) and low calcination temperature (<1123 K).

Agglomeration problems in the CLC unit can be detected by pressure drop measurements. If agglomeration occurred, the gas flow passed through preferential pathways drastically decreasing the bed pressure drop, and reducing the amount of active oxygen-carrier material. However, in spite of that the high operation temperatures used in the experiments, agglomeration or defluidization of the reactors (FR or AR) were never detected. SEM micrographs of used samples extracted at the end of the experiments from both FR and AR confirmed that individual particles maintained their original shape without formation of bridges between particles. Figure 4 shows that no substantial morphological changes were detected and particles remained individually, even in the experiment carried out at the highest temperatures (T_{FR} =1173 K, and T_{AR} = 1223 K). These results are relevant for the future use of Cu-based materials as oxygen carrier for CLC technology.

3.2.2. Attrition rates

Attrition and/or fragmentation of particles were analyzed during continuous long-term tests at high temperature. Abrasive attrition and fines generated from the fragmentation of particles are two possible mechanisms of fines generation that can occur in fluidised beds. The occurrence of fragmentation can be deduced from changes in the particle size distribution (PSD) of the samples recovered from the CLC system during each long-term test. Figure 5 shows the particle size distribution of both fresh and particles extracted from the reactors at the end of the different tests. It can be seen that all used particles do not exhibit much evidence of fragmentation, thereby indicating that any fines are generated primarily by abrasive attrition.

Particles elutriated from the fluidized bed reactors during operation were recovered in the filters and weighted to determine the attrition rate. The loss of fines was defined as the loss of particles smaller than 40 μm (Lyngfelt et al., 2005b). Particles of sizes >40 μm recovered in the filters were recycled into the system.

Attrition rate (A), was defined by Eq. (3), where w_f is the weight of elutriated particles < 40 μm during a period of time, w_t is the weight of total solids inventory and Δt is a period of time during the particles were collected.

$$A = \frac{w_f}{w_t . \Delta t} 100 \qquad (3)$$

Attrition rate is a useful measure to estimate the lifetime of particles. Fig. 6 shows the evolution with time of the attrition rate during the operation in the pilot plant at different temperatures (tests 1-4). The generation of fine particles was high at the beginning of the operation for all the tests but, after 20 h of operation a low value of the attrition rate was reached for tests 1, 2 and 3. However, for test 4 and after some combustion period for tests 2 and 3 (20, 38 and 42 h, respectively), an abrupt increase of the generation of fines was detected. These

values were too high and forced to stop operation in the CLC unit. It can be seen from Fig. 6 that only at operating conditions of test 1 (T_{FR} = 1073 K and T_{AR} = 1173 K) the system was running satisfactorily during more than 60 h with a moderate value of the attrition rate (0.09%), giving a particle lifetime of 1100 h. The particle lifetime of this Cu-based OC, Cu14Al, calculated after 100 h of operation in a 10 kW_{th} unit at T_{FR} = 1073 K and T_{AR} = 1073 K was about 2400 h (de Diego et al., 2007).

It was found that both T_{FR} and T_{AR} has a great influence on the attrition rate of the oxygen carrier. Increasing FR temperature from 1073 K to 1173 K, keeping T_{AR} = 1173 K, forced to stop operation at 48 h (test 3). Moreover, increasing T_{AR} from 1173 K to 1223 K, keeping T_{FR} = 1073 K, required to end the test at 42 h (test 2).

As can be inferred from these results, an increase of 100 K in the AR temperature operation can be done without an important detrimental of the OC costs. The reasons of the high attrition rates obtained when T_{FR} or T_{AR} were increased far from T_{FR} = 1073 K and T_{AR} = 1173 K will be discussed later.

3.2.3. Reactivity

Since in every cycle of CLC process the oxygen carrier undergoes important chemical and structural changes at high operating temperature, substantial changes in the reactivity with the number of cycles might be expected. In a previous work, Adánez et al. (2006) using Cu14Al particles in a 10 kW_{th} unit operated at lower temperatures (T_{FR} = 1073 K and T_{AR} = 1073 K) measured a loss of CuO content in the particles taken at the outlet of the AR as the operational time increased. In this work, the CuO content in the particles recovered in the filters and in samples taken at the outlet of the riser during operation was determined in TGA using H_2 as reducting gas. The CuO content in the particles recovered in the filters was significantly higher than the one corresponding to fresh oxygen carrier particles and it was changing with the operating time. At the beginning, the CuO loss was high, the CuO content in the fines were

around 75 % after 10 h of operation; however, this rate rapidly decreased to 0.2 wt % h^{-1} after 30 h, and the CuO content in the fines decreased until ~ 25 % at the end of each tests. On the other hand, the CuO content of the samples taken at the outlet of the riser decreased as the operation time increased for all the temperatures used. After 63 h of operation (test 1), the CuO content of the oxygen carrier was 11.8 wt %. Figure 7 shows the oxygen transport capacity ($R_{o,OC}$) versus time during reactivity test obtained in TGA at 1073 K, using a mixture of 15 vol %CH_4, 20 vol % H_2O, and 65 vol % N_2 in the fresh oxygen carrier and in samples taken at the end of the different tests, corresponding also to different operation times.

As can be observed, a decrease in the final value of the oxygen transport capacity was obtained as the operation time in the CLC plant increased, independently of the operation temperatures. This decrease was due to the decrease in the CuO content in the oxygen carrier particles, as noted previously. These results agreed with those found by Adánez et al. (2006), which attributed the copper lost to the erosion of the CuO grains present in the external surface of the fresh particles. Similar reason can be adduced here.

In spite of the reduction in the oxygen transport capacity, after-used Cu14Al particles showed high reactivities both in reduction and oxidation steps. Moreover, some minor differences in the reduction reactivities were observed for samples with the longest operation time (tests 1 and 2). In all cases, the used particles were highly reduced before 60 s, and showed similar and very high oxidation reactivities, indicating that particles maintain high reactivity after operation at high temperatures in the CLC pilot plant.

3.2.4. Characterization of Cu-based oxygen carrier

To analyze the results obtained regarding the effect of FR and AR temperatures on the behaviour of the particles, physical and chemical properties of the oxygen carrier particles coming from the AR, and from fines recovered in the filters at the FR and AR outlet streams were

compared to those of fresh particles. Table 1 shows the main properties of different after used samples in the CLC continuous unit of 500 W_{th} during long-term tests 1 to 4.

Figure 8 shows the pore size distribution of the fresh and after used oxygen carriers at different combustion times (10 h, 20 h, and end of test) for all the tests carried out. It can be seen that, after 10 hour of operation, the pore size distribution of the different samples has changed considerably with respect to the fresh particles. The respective mean pore size shifted towards pores of higher size, independently of the temperatures used. At the end of the tests, the pore size distribution of the different samples was very similar, indicating the presence of macro pores inside the particles, which was more noticeable when T_{AR} was increased. These results indicates that both the operating time and the reactor temperature affected to the pore size distribution.

The BET specific surface area decreased from 91.3 m^2/g in the fresh particles to less than 10 m^2/g after being used for all the samples. This important decrease for all samples suggest that important thermal sintering occurred in the particles due to the high operational temperatures used in FR and AR. The oxygen carrier bulk density presents a minor increase for all the tests, except for the highest temperature experiment (T_{FR} = 1173 K and T_{AR} = 1223 K), where the density decreased.

The evolution with time of the crushing strength of the particles at different operation temperatures was measured using samples extracted from the riser. Fig. 9 shows the effect of the operating temperature on the crushing strength at different operation times. It can be seen a fast and important decrease of this property at T_{FR} = 1173 K and T_{AR} = 1223 K. Both FR and AR temperatures has an important effect on the crushing strength evolution of the particles. Although the relation between crushing strength and particle lifetime is not established, it is believed that values considerably lower than 1N might be too soft for long-time circulation (Johansson et al., 2004). Moreover, in spite of the final crushing strength of the particles in test 2 (T_{FR} = 1073 K and T_{AR} = 1223 K) was 1.8 N, the attrition rate was very high and operation was stopped after 42 h.

Therefore, the initial and final values of the crushing strength of the OC particles are not a suitable characteristic to evaluate the particle lifetime in the process. As it was found in this work, the operation conditions strongly affect to the fluidization behaviour of the OC.

Powder XRD patterns of the fresh carriers, shown in Table 1, revealed the presence of CuO, $CuAl_2O_4$ and γ-Al_2O_3 as the crystalline phases for fresh Cu14Al. The powder XRD patterns of the used samples revealed the transformation of γ-Al_2O_3 to α-Al_2O_3 as a most stable phase at high temperature, explaining the observed evolution of the textural properties of the used particles. The interaction of copper with the support is revealed through the formation of copper aluminates ($CuAlO_2$ and $CuAl_2O_4$) that are present in the used particles both in particles extracted from the reactors and in fines recovered from the filters. Reduced CuO phases, Cu_2O and Cu, were detected in the samples collected in the filter at the outlet of the FR. Oxidized compounds of copper (CuO and copper aluminates) were only found in the samples coming from the AR and from the AR filter, verifying that the oxygen carrier reached always full oxidation state in the AR.

As it can be seen, similar crystalline phases to the fresh sample were detected in all used samples, independently of the different operating conditions. This fact revealed that the attrited material is composed as much of copper oxide as of support (Al_2O_3). However, a new phase was found in used samples ($CuAlO_2$), both in oxidized and reduced samples. The formation of this copper aluminate in air atmosphere is favoured as temperature increases (Bolt et al., 1998). However, it is unstable at temperatures below 1273 K, and may decompose by chemical reaction following (Susnitzky and Carter, 1991):

$$8CuAlO_2 + O_2 \rightarrow 4CuAl_2O_4 + 2\,Cu_2O \quad (4)$$

$$4CuAlO_2 + O_2 \rightarrow 2CuAl_2O_4 + 2\,CuO \quad (5)$$

The formation and dissociation of this metastable compound in particles operated at high temperatures might increase the erosion and attrition of the particles. Moreover, this copper aluminate was not previously detected in samples after 100 h of operation in a 10 kW_{th} unit operated at lower temperatures (T_{FR} = 1073 K and T_{AR} = 1073 K) using a similar OC (de Diego et

al. 2007). Therefore, it can be inferred that a support with a minimized interaction with the metal might be advantageous to increase the temperature resistance of copper-based oxygen carriers.

Finally, samples extracted from the AR at different operation times were also analyzed by SEM to determine changes produced in the structure of the solid materials during operation. Moreover, some particles were embedded in resin, cut, polished and analyzed by EDX. Images of cross section of fresh and after used particles at different tests and operation times are shown in Figure 10. Fresh Cu14Al particles exhibited an outer shell of CuO, although this layer disappeared, corroborated by the EDX analysis(white spots were Cu, during the first hours of operation by attrition. This fact qualitatively agrees with the CuO loss observed in the particles during operation. As it was showed in Table 1, the CuO content of the particles decreased from 14.2 % in the fresh particles to about 11.8 wt% after 63 h of operation at high temperature.

Samples of used Cu14Al particles presented important changes both in integrity and CuO grain dispersion depending on the temperatures used. At the lower temperatures, T_{FR} = 1073 K and T_{AR} = 1173 K, the small CuO grains are dispersed throughout the entire matrix, which was corroborated with an EDX profile. An increase in AR temperature produces an increase in the CuO grain size by sinterization of copper. At the highest temperature, T_{FR} = 1173 K and T_{AR} = 1223 K, OC particles have started to break apart, forming fines. Although the exact mechanism of formation of these structural defects is unidentified, the sintering of copper and the formation of the metastable $CuAlO_2$ compound could help to chunk the particles.

4. Conclusions

Long-term tests in a CLC continuous unit of 500 W_{th} using methane as fuel and CuO-γAl_2O_3 as oxygen carrier at temperatures of 1073 – 1173 K in FR and 1173 – 1223 K in AR were carried out. Changes in particles with respect to reactivity, chemical composition and physical characteristic were studied. The influence of the reactors temperature and solids circulation rate on combustion efficiency, gas products distribution, agglomeration, and attrition rate was

investigated. A total of about of 216 h in hot conditions were carried out, of which 182 h corresponded at combustion conditions with methane.

Complete fuel combustion was reached at ϕ > 1.4 or 1.2 when T_{FR} is 1073 K or 1173 K respectively. T_{AR} has a negligible effect on the combustion efficiency. It was found that Cu14Al particles maintained high reactivity after operation. Moreover, agglomeration or defluidizations of the reactors (FR or AR) were never detected in any of the tests.

Both T_{FR} and T_{AR} has a great influence on the temperature resistance of the particles in the long-term tests. The crushing strength of the OC particles was found to be an insufficient characteristic to evaluate the particle lifetime in the process. At T_{FR}=1073 K and T_{AR}=1173 K the system was running satisfactorily during more than 60 h, with an attrition rate of 0.09%.

Although the exact mechanism of formation of fines was unidentified, the sintering process of copper and the formation and dissociation of a copper aluminate compound, could increase the erosion and attrition of the particles. A support with a minimized interaction with the metal might be advantageous to increase the temperature resistance of copper-based oxygen carriers.

Cu-based OC have always been rejected as best candidate for the CLC process due to its agglomeration problems and its restricted operational temperatures. The results found in this work show that working with CuO-γAl_2O_3 as oxygen carrier an increase in the oxidation temperature from 1073 K to 1173 K is feasible, increasing in this way the net plant efficiency. However, a reduction in the particle lifetime from 2700 to 1100 h would be produced. Operational costs related with the oxygen carrier renovation should be taken into account.

This is the first time that a CuO-γAl_2O_3 OC, prepared by a commercial manufacturing method, and used at 1073K in the FR and 1173 K in the AR exhibits such a good properties: high reactivity together with high mechanical durability and absence of agglomeration. This result

opens new possibilities for the application of Cu-based materials in industrial-scale CLC processes.

ACKNOWLEDGEMENTS

This research was conducted with financial support from the Spanish Ministry of Science and Innovation (MICINN, Project CTQ2007-64400) and C.S.I.C. (200480E619).

REFERENCES

Abad, A., Adánez, J., García-Labiano, F., de Diego, L.F., Gayán, P., Celaya, J., 2007. Mapping of the range of operational conditions for Cu-, Fe-, and Ni-based oxygen carriers in chemical-looping combustion. Chem. Eng. Sci. 62, 533-549.

Adánez, J., de Diego, L. F., García-Labiano, F., Gayán, P., Abad, A., 2004. Selection of oxygen carriers for chemical-looping combustion. Energy Fuels 18, 371-377.

Adánez, J., Gayán, P., Celaya, J., de Diego, L.F., García-Labiano, F., Abad, A., 2006. Chemical-looping combustion in a 10 kW prototype using a CuO/Al_2O_3 oxygen carrier: effect of operating conditions on methane combustion. Ind. Eng. Chem. Res. 45, 6075-6080.

Anheden, M., Svedberg, G., 1998. Exergy analysis of chemical-looping combustion systems. Energy Convers. Mgmt. 39, No 16-18, 1967-1980.

Bolt, P. H., Habraken, F. H. P. M., Geus, J. W., 1998. Formation of nickel, cobalt, copper, and iron aluminates from α- and γ-alumina-supported oxides: A comparative study. Journal of Solid State Chemistry 135, 59-69.

Brandvoll, O., Bolland, O., 2004. Inherent CO_2 capture using chemical looping combustion in a natural gas fired power cycle. Journal of engineering for gas turbines and power. Transactions of the ASME, vol.126, 316-321.

Copeland, R. J., Alptekin, G., Cesario, M., Gershanovich, Y., 2002. Sorbent energy transfer system (SETS) for CO_2 separation with high efficiency. 27th International Technical

Conference on Coal Utilization & Fuel Systems, CTA: Clearwater, Florida, USA, March 4-7, vol. 2, 719-729.

Cho, P., Mattisson, T., Lyngfelt, A., 2004. Comparison of iron-, nickel-, copper-, and manganese-based oxygen carriers for chemical-looping combustion. Fuel 83, 1215-1225.

de Diego, L. F., García-Labiano, F., Adánez, J., Gayán, P., Abad, A., Corbella, B. M., Palacios, J. M., 2004. Development of Cu-based oxygen carriers for chemical-looping combustion. Fuel 83, 1749-1757.

de Diego, L. F., Gayán, P., García-Labiano, F., Celaya, J., Abad, A., Adánez, J., 2005. Impregnated CuO/Al_2O_3 oxygen carries for chemical-looping combustion: avoiding fluidized bed agglomeration. Energy Fuels 19, 1850-1856.

de Diego, L.F., García-Labiano, F., Gayán, P., Celaya, J., Palacios, J.M., Adánez, J., 2007. Operation of a 10 kW_{th} chemical-looping combustor during 200 h with a $CuO-Al_2O_3$ oxygen carrier. Fuel 86, 1036-1045.

Forero, C. R., Gayán, P., de Diego, L. F., Abad, A., García-Labiano, F., Adánez, J., 2009. Syngas combustion in a 500 W_{th} chemical-looping combustion system using an impregnated Cu-based oxygen carrier. Fuel Process. Technol. 90, 1471-1479.

Forero, C. R., Gayán, P., García-Labiano, F., de Diego, L. F., Abad, A., Adánez, J., 2010. Effect of gas composition in chemical-looping combustion with copper-based oxygen carriers: Fate of sulphur. Int. J. Greenhouse Gas Control 4, 762-770.

García-Labiano, F., de Diego, L. F., Adánez, J., Abad, A., Gayán, P., 2004. Reduction and oxidation kinetics of a copper-based oxygen carrier prepared by impregnation for chemical-looping combustion. Ind. Eng. Chem. Res. 43, 8168-8177.

García-Labiano, F., Gayán, P., Adánez, J., de Diego, L. F., Forero, C.R., 2007. Solid waste management of a chemical-looping combustion plant using Cu-based oxygen carriers, Environ. Sci. Technol. 41, 5882 -5887.

Gayán, P., Forero, C. R., de Diego, L. F., Abad, A., García-Labiano, F., Adánez, J., 2010. Effect of gas composition in chemical-looping combustion with copper-based oxygen carriers: Fate of light hydrocarbons. Int. J. Greenhouse Gas Control. 4, 13-22.

Intergovernmental Panel of Climate Change, 2007. Mitigation of climate change. Contribution of working group III to the fourth assessment report of the Intergovernmental panel on climate change. Cambridge University Press, Cambridge, U.K, 2008, (available at http://www.ipcc.ch).

Ishida, M., Jin, H., 1994. A new advanced power-generation system using chemical-looping combustion. Energy 19(4), 415-422.

Jin, H., Ishida, M., 2000. Investigation of a novel gas turbine cycle with coal gas fueled chemical-looping combustion. American Society of Mechanical Engineers – AES vol. 40, (Proceedings of the ASME Advanced Energy Systems Division-2000), 547-552.

Johansson, M., Mattisson, T., Lyngfelt, A., 2004. Investigation of Fe_2O_3 with $MgAl_2O_4$ for chemical-looping combustion. Ind. Eng. Chem. Res. 43, 6978-6987.

Kerr, H.R., 2005. Capture and separation technologies gaps and priority research needs. In: Thomas, D., Benson, S. (Eds.), Carbon Dioxide Capture for Storage in Deep Geologic Formations-Results from the CO_2 Capture Project, vol 1. Elsevier Ltd., Oxford, UK (Chapter 38).

Kolbitsch, P., Bolhàr-Nordenkampf, J., Pröll, T. and Hofbauer; H. 2009a. Comparison of two Ni-based oxygen carriers for chemical looping combustion of natural gas in 140 kW continuous looping operation. Ind. Eng. Chem. Res. 48, 5542-5547.

Kolbitsch, P., Pröll, T., Bolhàr-Nordenkampf, J., Hofbauer, H., 2009b. Operating experience with chemical looping combustion in a 120kW dual circulating fluidized bed (DCFB) unit. Energy Procedia 1, 1465-1472.

Kvamsdal, H., Jordal, K., Bolland, O., 2007. A quantitative comparison of gas turbine cycles with CO_2 capture. Energy 32, 10-24.

Kuusik, R., Trikkel, A., Lyngfelt, A., Mattisson, T., 2009. High temperature behavior of NiO-based oxygen carriers for chemical looping combustion. Energy Procedia 1, 3885-3892.

Lyngfelt, A., Thunman, H., 2005a. Construction and 100 h operational experience of a 10-kW chemical-looping combustor. In: Thomas, D., Benson, S. (Eds.), Carbon Dioxide Capture for

Storage in Deep Geologic Formations-Results from the CO_2 Capture Project, vol. 1. Elsevier Ltd., Oxford, UK (Chapter 36).

Lyngfelt, A., Kronberger, B., Adánez, J., Morin, J-X., Hurst, P., 2005b. The Grace Project. Development of oxygen carrier particles for chemical-looping combustion, design and operation of a 10 kW Chemical-looping combustor. In: Rubin, E.S., Keith, D.W., Gilboy, C.F. (Eds.). Proc. of the Seventh International Conference of Greenhouse Gas Control Technologies, vol. 1. Elsevier Ltd., Oxford, UK, p. 115.

Linderholm, C., Abad, A., Mattisson, T., Lyngfelt, A., 2008. 160 hours of chemical-looping combustion in a 10 kW reactor system with a NiO-based oxygen carrier. Int. J. of Greenhouse Gas Control 2, 520-530.

Naqvi, R., Bolland, O., 2007. Multi-stage chemical-looping combustion (CLC) for combined cycles with CO_2 capture. Int. J. Greenhouse Gas Control 1, 19-30.

Rydén M, Lyngfelt A, Schulman A, de Diego LF, Adánez J, Ortiz M, Pröll T, Bolhàr-Nordenkampf J, Kolbitsch P., 2009. Developing chemical looping steam reforming and chemical looping autothermal reforming. In: Eide LI, editor. Carbon dioxide capture for storage in deep geological formations– Results from the CO_2 capture project, UK: CPL Press; vol. 3. (Chapter 14).

Ryu, H.J., Jin, G.T., Yi, C.K., 2005. Demonstration of inherent CO_2 separation and no NO_x emission in a 50 kW chemical-looping combustor: continuous reduction and oxidation experiment. In: Wilson, M., Morris, T., Gale, J., Thambibutu, K. (Eds.). Proc. of the Seventh International Conference of Greenhouse Gas Control Technologies, vol. 2. Elsevier Ltd., Oxford, UK, p. 1907.

Ryu, H.-J., Jo, S-Ho, Park, Y.C, Bae, D.-H., Kim, S.D., 2010. Long-term operation experience in a 50 kW_{th} chemical looping combustor using natural gas and syngas as fuels. Proceedings of 1st International Conference on Chemical Looping. Lyon - Francia, 17-19 de marzo.

Susnitzky, D., Carter, B., 1991. The formation of copper aluminate by solid-state reaction. J. Mater. Res. 6, 1958-1963.

Tables

Table 1. Properties of the fresh and after used particles of Cu14Al at different pair FR-AR temperatures.

Table 2. Experimental conditions of the long-term tests in the CLC continuous unit of 500 W_{th}.

Table 1. Properties of the fresh and after used particles of Cu14Al at different FR and AR temperatures.

	Fresh	**After used**			
		$T_{FR} - T_{AR}$	**$T_{FR} - T_{AR}$**	**$T_{FR} - T_{AR}$**	**$T_{FR} - T_{AR}$**
Operating temperatures		**1173-1223**	**1073-1223**	**1173-1173**	**1073-1173**
Combustion time		**29 h**	**42 h**	**48 h**	**63 h**
CuO content (wt%)	14.2	13	12.8	12.7	11.8
Oxygen transport capacity $R_{o,OC}$ (%)	2.86	2.62	2.57	2.55	2.37
Mean particle size (μm)	401	379	370	371	373
Porosity (%)	50	58	50.5	54.8	45.4
Specific surface area BET (m^2/g)	91.3	6.8	5.3	3.9	9.2
Bulk density (g/cm^3)	1.7	1.5	1.8	1.8	2.1
Crushing strength (N)	2.9	0.6	1.8	1.3	2.1
Crystalline phases, particles from AR					
	CuO	CuO	CuO	CuO	CuO
	$CuAl_2O_4$	$CuAl_2O_4$	$CuAl_2O_4$	$CuAl_2O_4$	$CuAl_2O_4$
			$CuAlO_2$	$CuAlO_2$	
	γAl_2O_3	αAl_2O_3	αAl_2O_3	αAl_2O_3	αAl_2O_3
Crystalline phases, particles from FR filter					
		Cu	Cu	Cu	Cu
		CuO	CuO		CuO
		Cu_2O			Cu_2O
		$CuAl_2O_4$	$CuAl_2O_4$		$CuAl_2O_4$
			$CuAlO_2$	$CuAlO_2$	
		αAl_2O_3	αAl_2O_3	αAl_2O_3	αAl_2O_3
Crystallite phases, particles from AR filter					
		CuO	CuO	CuO	CuO
		$CuAl_2O_4$	$CuAl_2O_4$		$CuAl_2O_4$
		$CuAlO_2$	$CuAlO_2$	$CuAlO_2$	$CuAlO_2$
		αAl_2O_3	αAl_2O_3	αAl_2O_3	αAl_2O_3

Table 2. Experimental conditions of the long-term tests in the CLC continuous unit of 500 W_{th}.

Test	T_{FR} (K)	T_{AR} (K)	ϕ [a]	CH_4 [b] (%)	$t_{combustion}$ (h)
1	1073	1173	1.0 - 1.4	25 - 35	63
2	1073	1223	1.0 - 1.6	20 – 30	42
3	1173	1173	1.0 - 1.2	30 – 35	48
4	1173	1223	1.0 - 1.4	25 - 35	29

[a] Oxygen carrier to fuel ratio defined by eq. (2) [b] N_2 was used for balance

Figure captions

Figure 1. Schematic diagram of the Chemical-Looping Combustion unit of 500 W_{th}.

Figure 2. Effect of oxygen carrier to fuel ratios, ϕ, on the combustion efficiency at different FR and AR temperatures.

Figure 3. Effect of the oxygen carrier to fuel ratios, ϕ, on the gas product distribution at different FR and AR temperatures.

Figure 4. SEM micrograph pictures of different used Cu14Al particles at different FR and AR temperatures after *n* h of operation in the CLC continuous unit of 500 W_{th}.

Figure 5. Particle size distributions of fresh and after used Cu14Al particles extracted from the bed at the end of the tests.

Figure 6. Attrition rates vs time of Cu14Al at different FR and AR temperatures.

Figure 7. Oxygen transport capacity, $R_{o,OC}$ vs. time curves for reduction and oxidation reactions of fresh and after-used Cu14Al particles at different FR and AR temperatures. Reduction: CH_4 = 15%, H_2O = 20%, N_2 = 65%. Oxidation: air. T=1073 K.

Figure 8. Pore size distributions of fresh and after used Cu14Al particles at different FR and AR temperatures and operation times.

Figure 9. Crushing strength evolution of Cu14Al particles used at different FR and AR temperatures.

Figure 10. SEM pictures of a cross section of fresh and after used Cu14Al particles at different pair FR-AR temperatures and operation times.

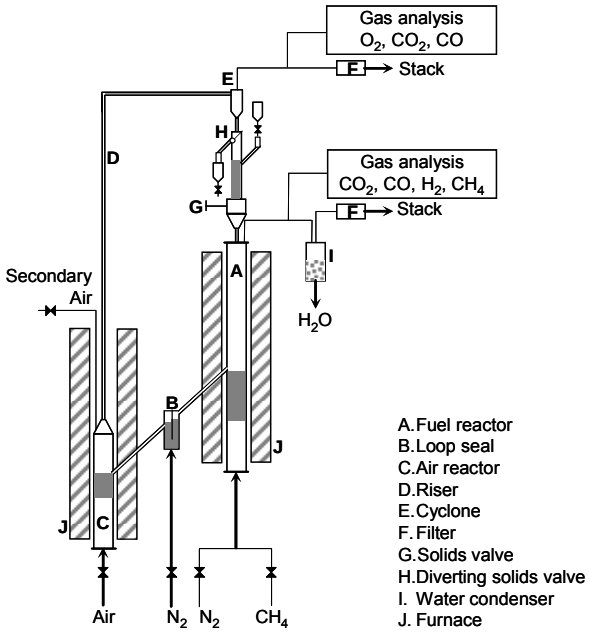

Figure 1. Schematic diagram of the Chemical-Looping Combustion unit of 500 W_{th}.

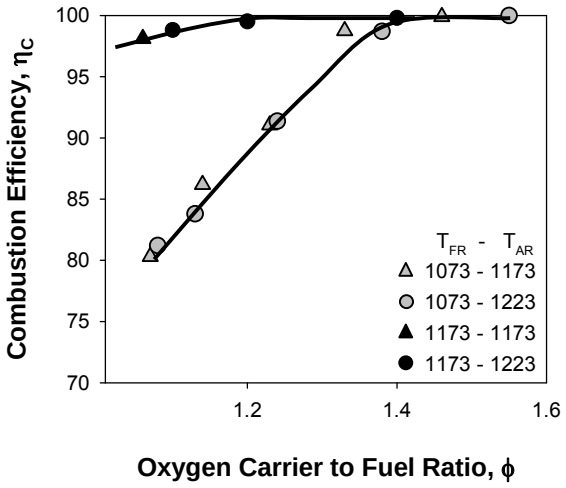

Figure 2. Effect of oxygen carrier to fuel ratios, ϕ, on the combustion efficiency at different FR and AR temperatures.

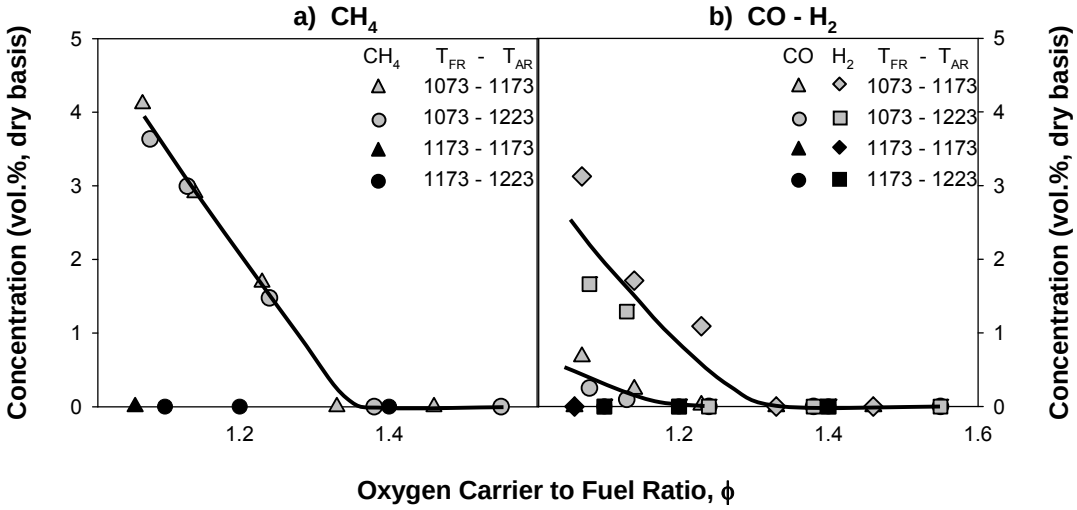

Figure 3. Effect of the oxygen carrier to fuel ratios, ϕ, on the gas product distribution at different FR and AR temperatures.

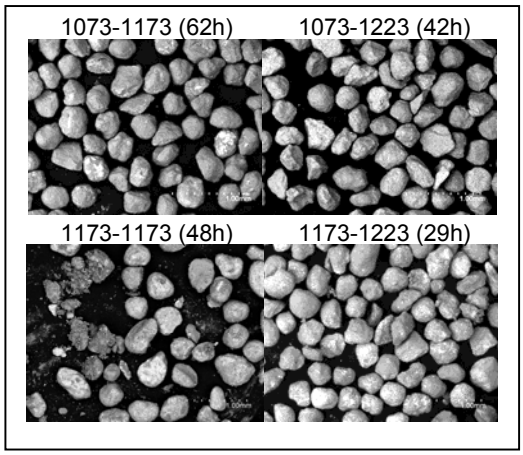

Figure 4. SEM micrograph pictures of different used Cu14Al particles at different FR and AR temperatures after *n* h of operation in the CLC continuous unit of 500 W_{th}.

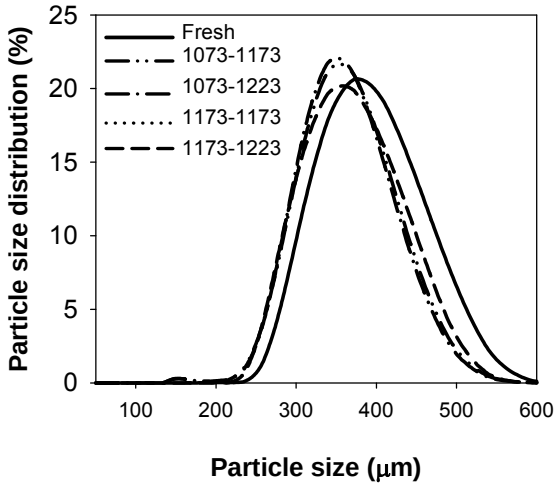

Figure 5. Particle size distributions of fresh and after used Cu14Al particles extracted from the bed at the end of the tests.

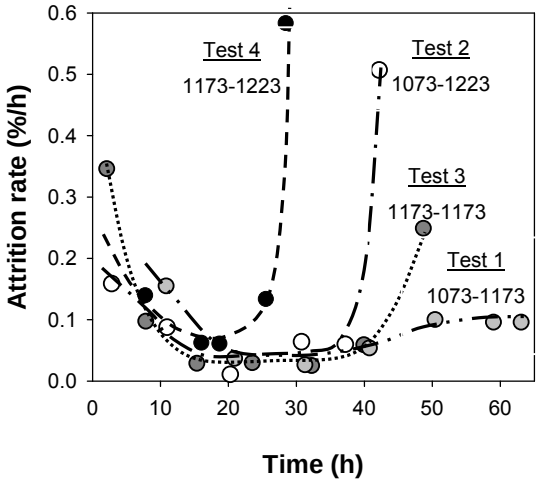

Figure 6. Attrition rates vs time of Cu14Al at different FR and AR temperatures.

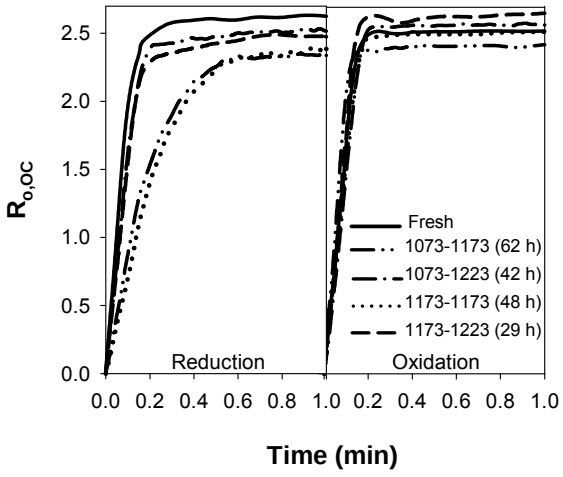

Figure 7. Oxygen transport capacity, $R_{o,OC}$ vs. time curves for reduction and oxidation reactions of fresh and after-used Cu14Al particles at different FR and AR temperatures. Reduction: CH_4 = 15%, H_2O = 20%, N_2 = 65%. Oxidation: air. T=1073 K.

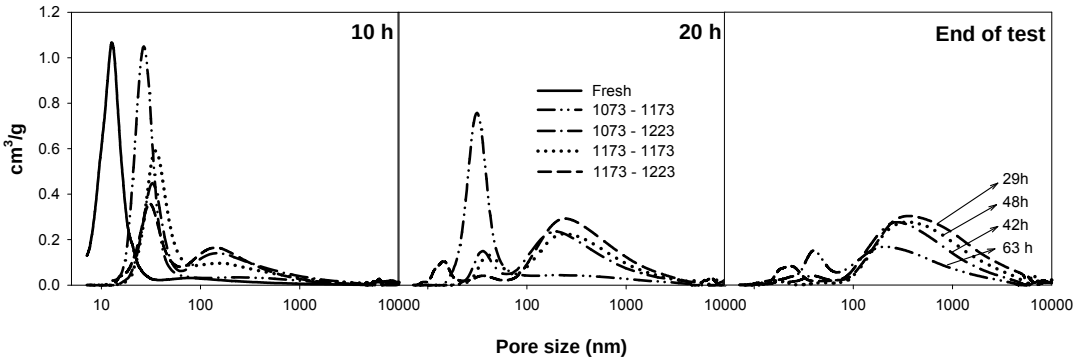

Figure 8. Pore size distributions of fresh and after used Cu14Al particles at different FR and AR temperatures and operation times.

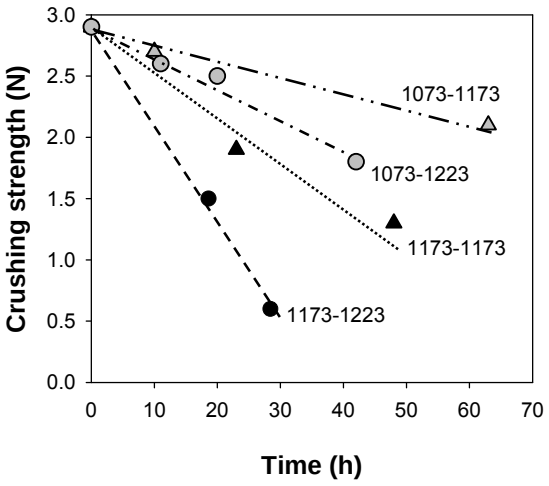

Figure 9. Crushing strength evolution of Cu14Al particles used at different FR and AR temperatures.

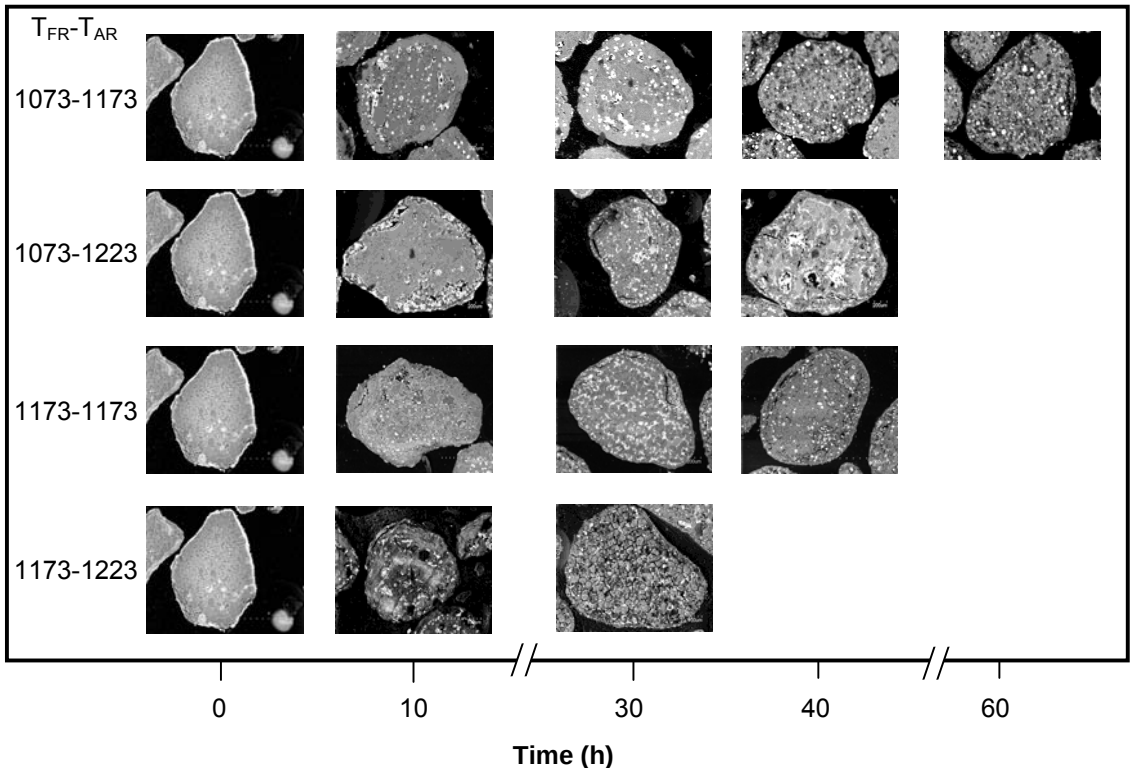

Figure 10. SEM pictures of a cross section of fresh and after used Cu14Al particles at different pair FR-AR temperatures and operation times.